Chapter 248

Modeling, Simulation, Motion Trajectory Planning and Nonlinear Control in the Joint Space of the Manipulator Robot SCARA T3 401SS Manufacturer Epson

https://doi.org/10.56238/devopinterscie-248

Flávio Luiz Rossini
Academico Department of Electrical Engineering, Federal University of Technology - Paraná (UTFPR)
Campus Campo Mourão Via Rosalina Maria dos Santos, 1233 CEP 87301-899 - Campo Mourão - Paraná - Brazil
E-mail: flrossini@utfpr.edu.br

Bruno Suracci de Lima
Academico Department of Electrical Engineering, Federal University of Technology - Paraná (UTFPR)
Campus Campo Mourão Via Rosalina Maria dos Santos, 1233 CEP 87301-899 - Campo Mourão - Paraná - Brazil
E-mail: bruno.suracci@gmail.com

João Henrique Dias Corrêa
Academico Department of Electrical Engineering, Federal University of Technology - Paraná (UTFPR)
Campus Campo Mourão Via Rosalina Maria dos Santos, 1233 CEP 87301-899 - Campo Mourão - Paraná - Brazil
E-mail: joao.henriquedias@hotmail.com

João Marcos Periçaro Lopes
Academico Department of Electrical Engineering, Federal University of Technology - Paraná (UTFPR)
Campus Campo Mourão Via Rosalina Maria dos Santos, 1233 CEP 87301-899 - Campo Mourão - Paraná - Brazil
E-mail: joaolopes@alunos.utfpr.edu.br

Reginaldo Ferreira de Sousa Barbosa
Academico Department of Electrical Engineering, Federal University of Technology - Paraná (UTFPR)
Campus Campo Mourão Via Rosalina Maria dos Santos, 1233 CEP 87301-899 - Campo Mourão - Paraná - Brazil
E-mail: reginaldobarbosa12@gmail.com

Yuri Ruzzene Barrozo
Acadêmico Department of Electrical Engineering, Universidade Tecnoló gicaFederal do Paraná – UTFPR
Campus Campo Mourão Via Rosalina Maria dos Santos, 1233 CEP 87301-899 - Campo Mourão - Paraná - Brazil
E-mail: yuriruzzenebarrozo@gmail.com

ABSTRACT
The paper proposed the mathematical modeling, trajectory planning, and nonlinear control of the manipulator robot SCARA T3 401SS manufacturer Epson. The National Confederation of Industry (CNI) developed a survey on the results of companies that have adopted Industry 4.0 concepts, and the results were released in 2018, which extensively use robots in their manufacturing plants. In Brazil, there are about 1,595 units with robots installed. Thus, the static and dynamic models of the robot were developed, which were used to carry out the trajectory planning and the nonlinear control system partitioned based on a model in the joint space. From this proposal, the code was constructed in the MATLAB® software environment. Then, the simulation was performed and the numerical results were obtained, regarding the position, speed, and acceleration of the effector about the fixed base of the robot, in the context of static and dynamic modeling. Through the mathematical description and computer simulation, the results proved to be coherent and promising, which have the purpose of contributing to students and professionals in the area who seek temporal models and behaviors, to check, compare and implement new embedded technologies. As well as evaluate the best performance of the robotic system.

Keywords: Scara T3 401SS Robot, Kinematic Modeling, Dynamic Modeling, Nonlinear Control System.

1 INTRODUCTION

Since 2010, the demand for industrial robots has increased considerably, due to the trend of automation and industrial technological innovation and the use of robotics, due to the emergence of the Industry 4.0 concept. After the drop in the number of robot installations in 2019, due to the trade war between China and the United States of America, the number of robot installations grew again in 2020, despite the global pandemic situation, and reached the number of 383,545 units installed. In Brazil, however, this number fell from 1,833 to 1,595 installed units [1].

Although Brazil is not among the largest consumers of robots in the world, as well as industrial plants installed, robotics is still an area that demands knowledge and development since the use of robotics is directly related to the competitiveness of the industry [1], in the face of the global market. According to the research of the National Confederation of Industry (CNI), companies that adopted the concepts of Industry 4.0 obtained better results than they had previously [2].

In certain situations, human intervention becomes limited or impossible, such as environmental conditions, physical disability, high accuracy of execution, force or movement scale factor, etc. In this way, the use of robotic systems becomes attractive, which emerges as a possible solution in the industrial environment. When considering the scale factor, the use of force in industrial applications stands out, as in the case of the manipulation of sheet metal bending equipment, used in the automotive industry. There are other applications of extreme precision, where the robot moves from the trajectory tracking, these being pre-established for the execution of the respective task. Thus, the use of robotic manipulators becomes attractive and motivates both the development of machines and the improvement of systems that aim to assist man in his design and development activities [3].

When considering the scenario of growth and application of robotics, there is a need to develop several fronts of this area, such as the theoretical field and front of design and construction of mechanisms. In the article [4], we presented the modeling of a PUMA robot with six degrees of freedom (dof) and the construction of an application for trajectory planning. In another article [5], the modeling, simulation, and trajectory control of a SCARA robot were shown. There are other articles, in which the authors have devoted themselves to laying the mathematical foundations of manipulative robots [6] [7] [8] [9] [10][11], as well as mobile robots with legs [12] [13].

In this context, the present article developed a case study applied to the Scara T3 401SS Manipulator Robot from the manufacturer EPSON [14]. From the lecture notes of the Introduction to Robotics course of the Electronic Engineering course at the Federal Technological University of Paraná (UTFPR), Campo Mourão Campus [15], the direct kinematics and robot dynamics were modeled, in addition to the application of a nonlinear position control strategy.

2 METHODS

Model Description

The SCARA robot model T3 401SS from the manufacturer Epson was considered for mathematical modeling, which includes the static model, represented by direct kinematics, and the dynamic description, in addition to the control strategy. All mathematical modeling and control were based on the CRAIG literature [16]. This robot has three degrees of freedom (dof), in which two joints are rotating and the last is prismatic, abbreviated by RRP or 2RP, illustrated in Figure 1.

To better infer the mathematical model, a two-dimensional mechanical scheme of the robot was developed, establishing the hypothesis of symmetry with the Xaxis, as illustrated in Figure 2. In this figure, the links and joints with the respective Reference Systems (RS)$\{i\}$, are observed, which $i = 1,2,3,4$, located at the origin of each link or rigid body of the robot.

A. RS Position$\{i\}$

In this subsection, the positions of the RS$\{i\}$ to the RS$\{i-1\}$ are presented, where $i = 1,2,3,4$. From the establishment of the RS$\{0\}$ as the origin and fixed, the other RS are mobile and were obtained as described:

$$^{0}P_{1} = [0 \quad 0 \quad h]^{T} \tag{1}$$

$$^{1}P_{2} = [0 \quad b \quad a]^{T} \tag{2}$$

Figure 1. Robot Epson model T3 401SS, Seiko Epson Corporation [17].

Figure 2. 2D mechanical model.

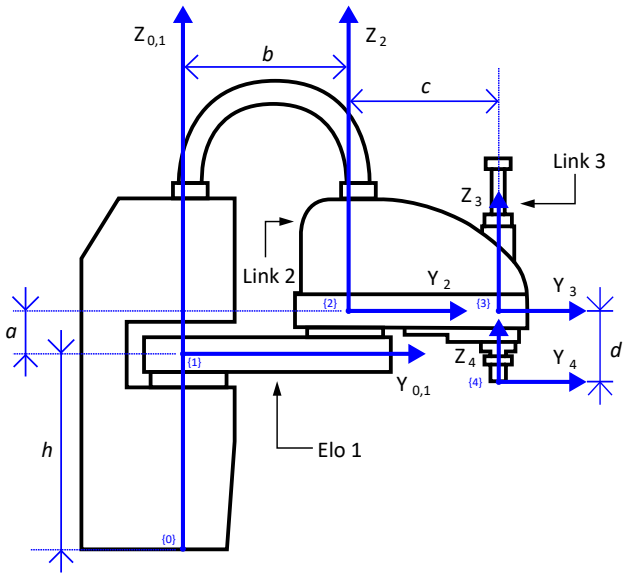

$$^{2}P_{3} = [0 \quad c \quad 0]^{T} \tag{3}$$

$$^{3}P_{4} = [\,0 \quad 0 \quad -d]^{T} \tag{4}$$

and d is the prismatic movement of the RS{*3*}.

RS{*i*} Guidance

For a full description of an RS, in addition to the position there is a need for the orientation of the mechanism. Thus, the projections of the RS{i} concerning the RS{$i - 1$}, were made $i = 1,2,3,4$, expressed as:

$$^{i-1}_{i}R = \begin{bmatrix} X_iX_{i-1} & Y_iX_{i-1} & Z_iX_{i-1} \\ X_iY_{i-1} & Y_iY_{i-1} & Z_iY_{i-1} \\ X_iZ_{i-1} & Y_iZ_{i-1} & Z_iZ_{i-1} \end{bmatrix} \tag{5}$$

The projection of the RS{1} about the RS{0} around the Z axis, expressed by:

$$^{0}_{1}R = \begin{bmatrix} c_1 & -s_1 & 0 \\ s_1 & c_1 & 0 \\ 0 & 0 & 1 \end{bmatrix} \tag{6}$$

being $cos(\theta_1) = c_1$ and $sen(\theta_1) = s_1$.

Analogously for the RS{2} about the RS{1} around the Z axis, obtained by:

$$ {}^{1}_{2}R = \begin{bmatrix} c_2 & -s_2 & 0 \\ s_2 & c_2 & 0 \\ 0 & 0 & 1 \end{bmatrix} \tag{7} $$

being $cos(\theta_2) = c_2$ and $sen(\theta_2) = s_2$.

In RS{3} concerning RS{2} prismatic motion occurs along the Z axis, so the rotational matrix is equal to the identity of order 3, given by:

$$ {}^{2}_{3}R = \begin{bmatrix} 1 & 0 & 0 \\ 0 & 1 & 0 \\ 0 & 0 & 1 \end{bmatrix} \tag{8} $$

Finally, the RS{4} about the RS{3} around the Z axis, the rotational matrix and obtained as:

$$ {}^{3}_{4}R = \begin{bmatrix} c_4 & -s_4 & 0 \\ s_4 & c_4 & 0 \\ 0 & 0 & 1 \end{bmatrix} \tag{9} $$

being $cos(\theta_4) = c_4$ and $sen(\theta_4) = s_4$

For a full description of the Direct Kinematics of the robot, the position vector, Eqs. (1)-(4), and the rotational matrix, Eqs. (6)-(9), of the respective RS should be concatenated in a single structure, called the Transformation Equation (TE). The general form of ET is given by:

$$ {}^{i-1}_{i}T = \begin{bmatrix} {}^{i-1}_{i}R & {}^{i-1}P_i \\ 0_{1x3} & 1 \end{bmatrix} \tag{10} $$

The following are listed the TEs for each link, Eq. (10), where $i = 1,2,3,4$, of the form:

$$ {}^{0}_{1}T = \begin{bmatrix} c_1 & -s_1 & 0 & 0 \\ s_1 & c_1 & 0 & 0 \\ 0 & 0 & 1 & h \\ 0 & 0 & 0 & 1 \end{bmatrix} \tag{11} $$

$$ {}^{1}_{2}T = \begin{bmatrix} c_2 & -s_2 & 0 & 0 \\ s_2 & c_2 & 0 & b \\ 0 & 0 & 1 & a \\ 0 & 0 & 0 & 1 \end{bmatrix} \tag{12} $$

$$ {}^{0}_{1}T = \begin{bmatrix} c_3 & -s_3 & 0 & 0 \\ s_3 & c_3 & 0 & c \\ 0 & 0 & 1 & 0 \\ 0 & 0 & 0 & 1 \end{bmatrix} \quad (13) $$

$$ {}^{3}_{4}T = \begin{bmatrix} c_4 & -s_4 & 0 & 0 \\ s_4 & c_4 & 0 & 0 \\ 0 & 0 & 1 & -d \\ 0 & 0 & 0 & 1 \end{bmatrix} \quad (14) $$

Kinematics

Kinematics is the area of knowledge that deals with the subject without considering the forces that cause it, this deals only with position, speed, acceleration over time and other derivatives, from geometry. In this step will be considered the positions and orientations of the RS of the robot in a static configuration, are to determine the position of the links concerning the RS{0}.

A. Direct Kinematics

The Direct Kinematics (CD), corresponds to the static mathematical description of the robot, this description has as independent variables and as dependent variables the cartesian position of the RS .

In order to locate the final effector, RS{4}, with the fixed base of the robot, RS{0}, the multiplication of the TEs, Eqs, was performed. (11)-(14), as follows:

$$ {}^{0}_{4}T = {}^{0}_{1}T({}^{1}_{2}T({}^{2}_{3}T\,{}^{3}_{4}T))) \quad (15) $$

The TE, shown in Eq. (15), has the structure of the form:

$$ {}^{0}_{4}T = \begin{bmatrix} {}^{0}_{4}R & {}^{0}P_4 \\ 0_{1x3} & 1 \end{bmatrix} \quad (16) $$

being by inspection it is possible to identify the equivalent rotational matrix, as well as the location of the robot effector, ${}^{0}P_4$.

Trajectory description

In this section, the trajectory of this robot was described, based on the use of Eq. (16).

The trajectory of the robot must have smooth movement, this is necessary so that the manipulator does not have sudden movements, which can lead to vibrations or damage to the system. To tend the restriction of smooth motion, the polynomial of the third degree was used, as follows:

$$\theta(t) = a_0 + a_1 t + a_2 t_2 + a_3 t_3 \quad (17)$$

where $\theta(t)$ is the value of the angle of the joint as a function of time t, a_i, where $i = 0,1,2,3$, are the parameters of the polynomial so that the motion is smooth.

The first derives from Eq. (17), which corresponds to the velocity equation of the mechanism, obtained by:

$$\dot{\theta}(t) = a_1 + 2a_2 t + 3a_3 t_2 \quad (18)$$

The derivative of Eq. (18), this being the acceleration equation, is expressed by:

$$\ddot{\theta}(t) = 2a_2 + 6a_3 t \quad (19)$$

Established of the Eqs. (17)-(19), then position and speed restrictions were imposed, such as:

$$\theta(0) = \theta_0 \quad (20)$$
$$\theta(tf) = \theta_f \quad (21)$$
$$\dot{\theta}(0) = 0 \quad (22)$$
$$\dot{\theta}(tf) = 0 \quad (23)$$

$t_f$being final time of movement, θ_0 initial angle and $\theta_f$final angle, in addition to the initial and final zero velocities.

To determine the parameters *ai*, with $i = 0,1,2,3$, the Eqs conditions were replaced Eqs. (20)-(23), in the Eqs. (17)-(19), when manipulating it was obtained:

$$a_0 = \theta_0 \quad (24)$$
$$a_1 = 0 \quad (25)$$
$$a_2 = \frac{3}{t_f^2}(\theta_f - \theta_0) \quad (26)$$
$$a_3 = -\frac{2}{t_f^3}(\theta_f - \theta_0) \quad (27)$$

From the given parameters, Eqs. (24)-(27), it becomes possible to perform the trajectory planning of the robot effector, as will be illustrated in the Results Section.

Dynamics

Dynamics is the area of knowledge that considers the forces necessary to cause movement. In this context there are two problems related to the dynamics of the robot, namely: (*i*) from a point of trajectory find the vector τ necessary for the torques of the joints; and (*ii*) with the torque vector τ find the trajectory of the robot.

A. Mass Distribution

To begin the study of motion, it becomes necessary to analyze the mass distribution of the links and consequently the inertia tensioners, which can be defined in relation to any RS{i}, where $i = 0,\ldots,4$. In the case of the SCARA robot, the RS of each link located in the Mass Center (MC) of the body was adopted, in addition to considering each body analogous to a cobblestone, massive and rigid. The MC can be expressed by:

$$\begin{bmatrix} x_{cm} \\ y_{cm} \\ z_{cm} \end{bmatrix} = \frac{1}{2}\begin{bmatrix} k \\ l \\ q \end{bmatrix} \tag{28}$$

where k is the length along the X_i axis, l is the width along the Y_i axis and q is the height along the Z_i , *whit i=1,...,4.*

The inertia tensor for each rigid body, $i = 1,2,3$, can be obtained by:

$${}^{c}I_i = \begin{bmatrix} \frac{mi}{12}\left(q_i^2 + l_i^2\right) & 0 & 0 \\ 0 & \frac{mi}{12}\left(k_i^2 + q_i^2\right) & 0 \\ 0 & 0 & \frac{mi}{12}\left(l_i^2 + k_i^2\right) \end{bmatrix} \tag{29}$$

being m the mass of the link.

B. Newton–Euler Iterative Dynamic Algorithm

To obtain the dynamic equations of the robot, the Newton-Euler iterative algorithm was applied. Thus, they determined whether the torque equations τ for each joint of the link robot $i = 0 \rightarrow n - 1$.

The angular velocity equation:

$$^{i+1}\omega_{i+1} = {}^{i+1}_{i}R\,{}^{i}\omega_i + \dot{\theta}_{i+1}\,{}^{i+1}\hat{Z}_{i+1} \quad (30)$$

where $^{i+1}\omega_{i+1}$ the angular velocity of the link $\{i + 1\}$ with respect to the RS$\{i + 1\}$ and $^{i+1}Z_{i+1}$ axis of rotation of the link $\{i + 1\}$, in this case .

The angular acceleration equation:

$$^{i+1}\dot{\omega}_{i+1} = {}^{i+1}_{i}R\,{}^{i}\omega_i + {}^{i+1}_{i}R\,{}^{i}\dot{\omega}_i \times \dot{\theta}_{i+1}\,{}^{i+1}\hat{Z}_{i+1} + \ddot{\theta}_{i+1}\,{}^{i+1}\hat{Z}_{i+1} \quad (31)$$

being $^{i+1}\dot{\omega}_{i+1}$ the angular acceleration of the link $\{i + 1\}$ concerning the RS$\{i + 1\}$.

The linear acceleration equation:

$$^{i+1}\dot{v}_{i+1} = {}^{i+1}_{i}R\,(\,{}^{i}\dot{\omega}_i \times {}^{i}P_{i+1} + {}^{i}\omega_i \times ({}^{i}\omega_i \times {}^{i}P_{i+1}) + {}^{i}\dot{v}_i) \quad (32)$$

being $^{i+1}\dot{v}_{i+1}$ the linear acceleration of the link $\{i + 1\}$ in relation to the RS$\{i + 1\}$.

The linear acceleration equation of MC:

$$^{i+1}\dot{v}_{ci+1} = {}^{i+1}\dot{\omega}_{i+1} \times {}^{i+1}P_{c_{i+1}} + {}^{i+1}\omega_{i+1} \times ({}^{i+1}\omega_{i+1} \times {}^{i+1}P_{c_{i+1}}) + {}^{i+1}\dot{v}_{i+1} \quad (33)$$

being $^{i+1}\dot{v}_{ci+1}$ the linear acceleration of the link $\{i + 1\}$ with respect to its MC and $^{i+1}P_{c_{i+1}}$ the position vector of the link $\{i + 1\}$ MC. The force equation:

$$^{i+1}F_{i+1} = m_{i+1}\,{}^{i+1}\dot{v}_{c_{i+1}} \quad (34)$$

where $^{i+1}F_{i+1}$ the force equation is relative to the RS$\{i + 1\}$.

The torque equation:

$$^{i+1}N_{i+1} = {}^{Ci+1}I_{i+1}\,{}^{i+1}\dot{\omega}_{i+1} + {}^{i+1}\omega_{i+1} \times {}^{Ci+1}I_{i+1}\,{}^{i+1}\omega_{i+1} \quad (35)$$

where $^{i+1}F_{i+1}$ the torque equation with respect to RS{i + 1} and $^{Ci+1}I_{i+1}$ the inertia tensor of the link $\{i + 1\}$.

For prismatic joints, one must use the equations corresponding to the eqs. (31) and (32), respectively:

$$^{i+1}\dot{\omega}_{i+1} = {}^{i+1}_{i}R\,{}^{i}\omega_i \tag{36}$$

$$^{i+1}\dot{v}_{i+1} = {}^{i+1}_{i}R\,(\,{}^{i}\dot{\omega}_i \times {}^{i}P_{i+1} + {}^{i}\omega_i \times (\,{}^{i}\omega_i \times {}^{i}P_{i+1}) + {}^{i}\dot{v}_i) + \cdots \tag{37}$$
$$\ldots 2\,{}^{i+1}\omega_{i+1} \times \dot{d}_{i+1}\,{}^{i+1}\hat{Z}_{i+1} + \ddot{d}_{i+1}\,{}^{i+1}\hat{Z}_{i+1}$$

After performing the iterations described by the Eqs. (31)-(35), Newton-Euler algorithm was finalized with the interactions of the link $i = n \rightarrow 1$, thus there was the decomposition of the torques τ_i.

The force equation:

$$^{i}f_i = {}^{i}_{i+1}R\,{}^{i+1}f_{i+1} + {}^{i}F_i \tag{38}$$

being $^{i}f_i$ the force in the joint $\{i\}$.

The torque equation:

$$^{i}n_i = {}^{i}N_i + {}^{i}_{i+1}R\,{}^{i+1}n_{i+1} + {}^{i}P_{Ci} \times {}^{i}F_i + {}^{i}P_{i+1} \times {}^{i}_{i+1}R\,{}^{i+1}f_{i+1} \tag{39}$$

being $^{i}n_i$ the torque in the joint $\{i\}$.

The decomposed torque equation on axis of rotation or translation:

$$\tau = {}^{i}n_i^T\,{}^{i}\hat{Z}_i \tag{40}$$

the τ_i torque being oriented in the joint $\{i\}$.

After performing the iterations out, Eqs. (31)-(35), and inward, Eqs. (38)-(40), the calculated torques for each joint are presented, τ_1 and τ_2 the torques performed on joints 1 and 2, respectively, and τ_3 the force applied to the prismatic joint:

$$\tau_1 = (m_1 b_{cm}^2 + {}^{c}I_{ZZ1})\ddot{\theta}_1 + (m_2(b^2 + 2bc_{cm}c^2 + c_{cm}^2) + {}^{c}I_{zz2})\ddot{\theta}_1 + \ldots$$
$$\ldots (m_2(bc_{cm}c^2 + c_{cm}^2) + {}^{c}I_{zz2})\ddot{\theta}_2 + (m_3(b^2 + 2bcc^2 + c^2) + {}^{c}I_{zz3})\ddot{\theta}_1 + \ldots \tag{41}$$
$$\ldots (m_3(bcc_2 + c^2) + {}^{c}I_{zz3})\ddot{\theta}_2$$

$$\tau_2 = (m_2(bc_{cm}c_2 + c_{cm}^2) + {}^cI_{zz2})\ddot{\theta}_1 + \ldots$$
$$\ldots (m_3(bcc_2 + c^2) + {}^cI_{zz3})\ddot{\theta}_1 + \ldots$$
$$\ldots (m_3c^2 + {}^cI_{zz3})\ddot{\theta}_2 + (m_2c_{cm}^2 + {}^cI_{zz2})\ddot{\theta}_2 + \ldots \quad (42)$$
$$\ldots (m_2bc_{cm}s_2)\dot{\theta}_1^2 + (m_2bc_{cm}s_2) + \dot{\theta}_1\dot{\theta}_2 \ldots$$
$$\ldots (m_3bcs_2)\dot{\theta}_1^2 + (m_3bcs_2) + \dot{\theta}_1\dot{\theta}_2$$

$$\tau_3 = m_3\ddot{d} - m_3g \quad (43)$$

can be suitable Eqs. (41)-(43) in the form of a general equation, expressed by:

$$\tau = M(\theta)\ddot{\theta} + V(\theta, \dot{\theta}) + G(\theta) \quad (44)$$

where τ is the torque vector, the ($n\times1$), $M(\theta)$ inertia matrix of the manipulator ($n\times n$), $V\ (\theta, \dot{\theta})$ is the vector of the Centrifugal and Coriolis ($n\times1$) terms and $G(\theta)$ is a vector of the terms Gravity (n×1). Note that the terms are dependent on θ (position), $\dot{\theta}$ (velocity), and $\ddot{\theta}$ (acceleration).

In the case of the robot SCARA model T3 401SS, the matrix of inérica, , $M(\theta)$, of Eq. (44) becomes:

$$A_1 = {}^cI_{zz1} + {}^cI_{zz2} + {}^cI_{zz3} + b_{cm}^2m_1 + \ldots \quad (45)$$
$$\ldots\ m_3(b^2 + 2bcc_2 + c^2) + m_2(b^2 + 2bc_{cm}c_2 + c_{cm}^2)$$

$$B_1 = {}^cI_{zz2} + {}^cI_{zz3} + m_3(c^2 + bcc_2) + m_2(c_{cm}^2 + bc_{cm}c_2) \quad (46)$$

$$C_1 = 0 \quad (47)$$

$$M_1 = [A_1 \quad B_1 \quad C_1] \quad (48)$$

$$A_2 = {}^cI_{zz2} + {}^cI_{zz3} + m_3(c^2 + bcc_2) + m2(c_{cm}^2 + bc_{cm}c_2) \quad (49)$$

$$B_2 = {}^cI_{zz2} + {}^cI_{zz3} + m_3c^2 + m_2c_{cm}^2 \quad (50)$$

$$C_2 = 0 \quad (51)$$

$$M_2 = [A_2 \quad B_2 \quad C_2] \quad (52)$$

$$A_3 = 0 \quad (53)$$

$$B_3 = 0 \quad (54)$$

$$C_3 = m_3 \tag{55}$$

$$M_3 = [A_3 \quad B_3 \quad C_3] \tag{56}$$

The matrix M will be composed of the Eqs. (48), (52) and (56), expressed as:

$$M = \begin{bmatrix} M_1 \\ M_2 \\ M_3 \end{bmatrix} \tag{57}$$

Analogously for the vector $V\ (\theta, \dot{\theta})$, Eq. (44), it is obtained:

$$V_1 = 0 \tag{58}$$

$$V_2 = (bcm_3 s_2 + bc_{cm} m_2 s_2)\dot{\theta_1^2} + (bcm_3 s_2 + bc_{cm} m_2 s_2)\dot{\theta}_1 \dot{\theta}_2 \tag{59}$$

$$V_3 = 0 \tag{60}$$

$$V = [V_1 \quad V_2 \quad V_3]^t \tag{61}$$

The last vector, $G(\theta)$, from Eq. (44), it is obtained:

$$G_1 = 0 \tag{62}$$

$$G_2 = 0 \tag{63}$$

$$G_3 = -gm_3 \tag{64}$$

$$G = [G_1 \quad G_2 \quad G_3]^t \tag{65}$$

To perform the simulation, it is necessary to isolate the variable $\ddot{\theta}$ from the Eq. (44), as follows:

$$\ddot{\theta} = M(\theta)^{-1}(\tau - V(\theta, \dot{\theta}) - G(\theta) \tag{66}$$

To perform the point-to-point iteration, the time to perform the numerical integration was discretized, starting from the Eq. (66), one obtains:

$$\dot{\theta} = \dot{\theta} + T_x\ddot{\theta} \tag{67}$$

$$\theta = \theta + T_x\dot{\theta} \tag{68}$$

where T_x the sampling rate is.

In the next section, Equation (44) will be used to control the manipulator robot.

Nonlinear Control

Once the dynamic modeling is completed, it is desired that the links of the manipulator robot follow certain trajectories. In this way, the torque control of the actuators is carried out in order to reach the desired final position smoothly.

There are control strategies applied to robotic manipulators, these can be classified as linear or non-linear. For the case of tenuous nonlinearities, local linearization becomes possible, linear models are obtained that approximate the nonlinear equations in the vicinity of the point of operation. However, the control problem of a manipulator robot is not suitable for this approach.

Therefore, we seek a control law that does not neglect the intrinsic nonlinearities of the robot so that the control system is critically dampened, being described by the open mesh system in Equation (44).

Figure 3. Closed-loop control diagram.

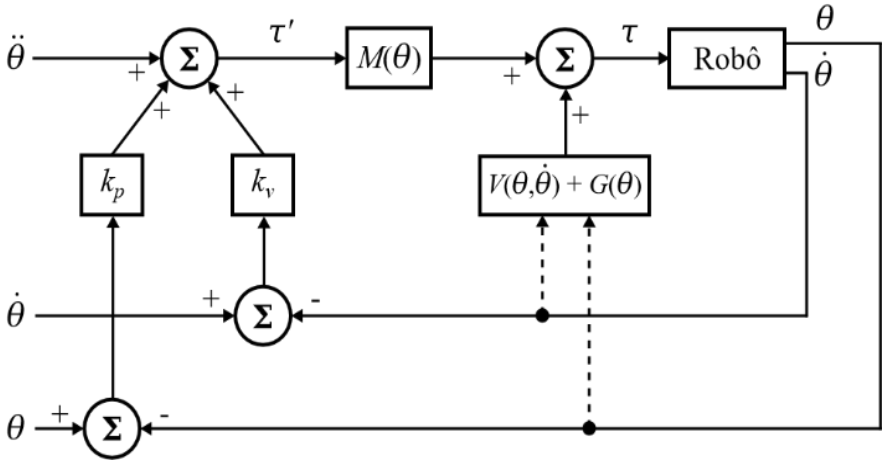

Source: Adapted from [16]

Figure 3 shows the closed-loop control diagram of the system.

The partition of the control law obtains the following model:

$$\tau = \alpha\tau' + \beta \tag{69}$$

where , $\alpha = M(\theta), \beta = V(\theta, \dot{\theta}) + G(\theta)$ and the τ' partition of the servo expressed by:

$$\tau' = \ddot{\theta} + k_v \dot{e} + k_p e \quad (70)$$

where k_p is the gain of position, k_v is the gain of speed, e is the error of position and $\dot{e}$ is the error of velocity, given by:

$$e = \theta_f - \theta_a \quad (71)$$

The speed error, $\dot{e}$, expressed by:

$$\dot{e} = \dot{\theta}_f - \dot{\theta}_a \quad (72)$$

being θ_f is the desired final position, θ_a the current position of the robot, $\dot{\theta}_f$ the desired final speed, $\dot{\theta}_a$ and the current speed of the robot. The parameters k_p and k_v, are calculated based on the performance specifications of the project.

As for the computational implementation, Eqs. (44) is discretized, then: *(i)* the variables of position (θ), velocity ($\dot{\theta}$) and acceleration ($\ddot{\theta}$); *(ii)* the errors of position (e) and velocity ($\dot{e}$), described in Eqs. (71)-(72); *(iii)* the partition of the servo is calculated (τ'), according to Eq. (70); and *(iv)* the open mesh equation is computed, according to Equation (69).

To implement the law of control, it isolated ($\ddot{\theta}$) in Equation (44), as follows:

$$\ddot{\theta} = \alpha^{-1}(-\beta + \tau) \quad (73)$$

At this stage of the iteration, numerical integration was performed and obtained ($\dot{\theta}$) and (θ), as expressed in Equations (67) and (68).

The variables $\dot{\theta}$ and θ of the iterative loop is returned until the stopping condition is reached.

3 RESULTS

The results were obtained from the MATLAB software®. Trajectory and control simulations were performed based on the desired position, velocity and acceleration values for each link, with the parameters presented in Table $i = 1,2,3$.

Table 1. Parameters used in the simulations.

Links	$i = 1$	$i = 2$	$i = 3$
m_i (Kg)	*1.2*	*4.0*	*0.4*
$MC_i(m)(10^{-3})$	112.5	87.5	*170.0*
$k_i(m)(10^{-3})$	90	129	8.57
$l_i(m)(10^{-3})$	225	175	8.57
$q_i(m)(10^{-3})$	35	176	*340.7*
${}^{c}_{Ixxi}$ (10−6)	10400	38100	3900
${}^{c}_{Iyyi}$ (10−6)	900	16000	3900
${}^{c}_{Izzi}$ (10−6)	11000	33300	4.8963
θ_i Initial (rad)	0	0	0
$\dot{\theta}_i$ Initial (rad/s)	0	0	0
θ_i Final (rad)	π	$-\pi$	0.15
$\dot{\theta}_i$ Final (rad/s)	0	0	0
$\ddot{\theta}_i$ Final (rad/s^2)	0	0	0
g (m/s^2)	*9.8*	*9.8*	*9.8*
k_{pi}	1	0.25	4
k_{vi}	2	1	4
T_{xi} (s)	0.001	0.001	0.001

A. Trajectory generation

The graph of the trajectory was generated, with the conditions presented in Eqs. (17)-(19), to determine the coefficients described in Eqs. (24)-(27). Figures 4-6 illustrate the temporal behaviors of the links $i = 1,2,3$.

Figure 4. Elo Trajectory 1, where position, velocity and acceleration, respectively.

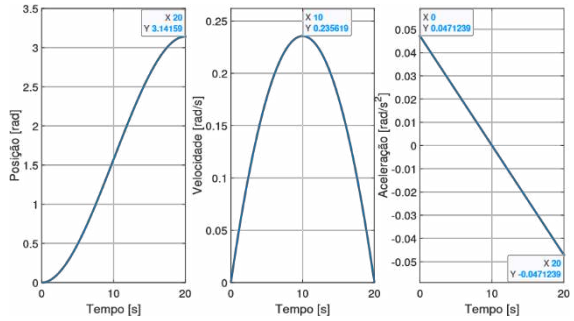

Figure 5. Elo Trajectory 2, where position, velocity and acceleration, respectively.

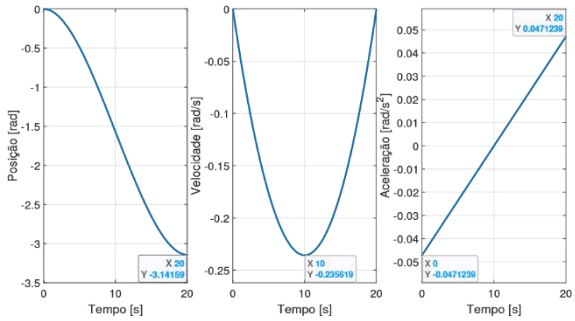

Figure 6. Elo Trajectory 3, where position, velocity and acceleration, respectively.

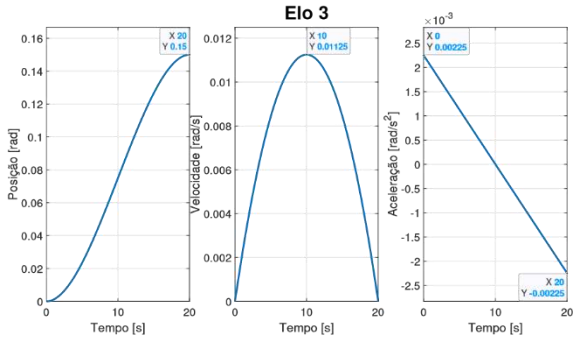

B. Control

In the control stage, the Eqs. (57), (61) and (65) were calculated, which compose the dynamics of the robot and composed the control system in the closed mesh. For simulation, the parameters presented in Table I and a sampling time of *0.001*s were used. Figures 7-9 illustrate the numerical results regarding the temporal behavior of the RRP robot links.

Figure 7. Control of position, speed, and acceleration of link 1.

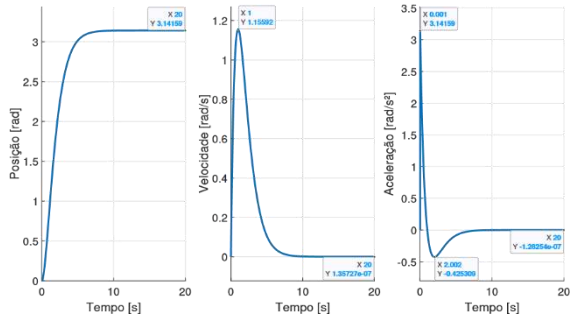

Figure 8. Control of position, speed, and acceleration of link 2.

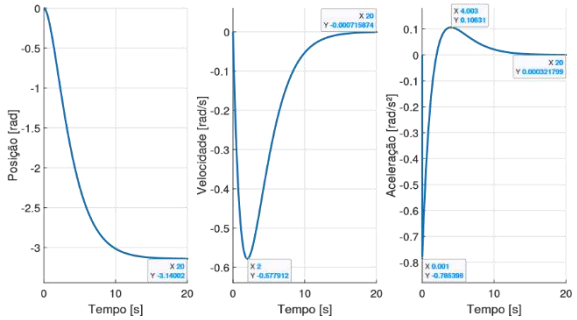

Figure 9. Control of position, speed, and acceleration of the link 3.

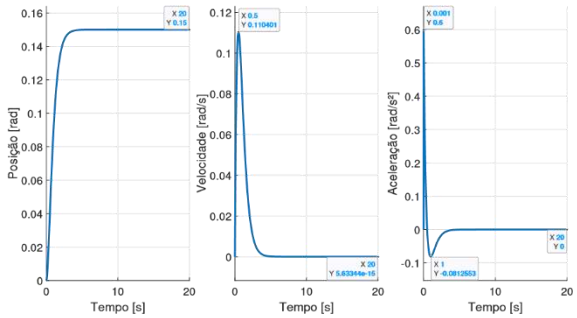

4 CONCLUSION

The present article developed the mathematical modeling of kinematics and dynamics of the SCARA T3 401SS Robot of the EPSON Company, as well as the trajectory planning and nonlinear control system. The dynamics were performed using the Newton–Euler iterative method, which provided the set of torque equations, which was later used to control the actuators.

The simulation and analysis of the position, velocity, and acceleration graphs of the joints were performed to verify the coherence of the results obtained, which were checked for the aforementioned manipulator robot.

The modeling was validated through the results, thus it was evidenced the possible use of this model for the simulation and design of robots with rotating joints and prismatic since the mathematical model is generic. In this way it allows the adaptation of the parameters of other robots with analogous structures, this helps professionals in the area of the theoretical verification of the results, before the application or even physical construction of the mechanism.

Therefore, it was noted the distinction between the simulated results and presented in Figures 4-6, as compared to the results illustrated in Figures 7-9, since the static and dynamic models are used, respectively.

REFERENCES

[1] IFR (1993-2021). World Robotics: Industrial Robots. Frankfurt am Main: VDMA Services GmbH, p. 12-14. Disponível em: <https://ifr.org/img/worldrobotics/Executive_Summary_WR_Industrial_Robots_2021.pdf> Acessado em 06 de julho de 2022

[2] CNI – Confederação Nacional da Indústria. Investimentos em indústria 4.0 / Confederação Nacional da Indústria. Brasília, 2018. Disponível em: <https://static.portaldaindustria.com.br/media/filer_public/8b/0f/8b0 f5599-9794-4b66-ac83-e84a4d118af9/investimentos_em_industria_40 _junho2018.pdf>. Acessado em 06 de julho de 2022

[3] CHAGAS, Fábio Suim. Manipulador Bilateral com Realização Háptica. 2005. Tese de Doutorado. Instituto Militar de Engenharia. Disponível em: <http://www.comp.ime.eb.br/pos/modules/files/dissertacoes/2005/2005FabioChagas.pdf> Acessado em 07 de julho de 2022.

[4] SOUZA, Eber Delgado de; ROSSINI, Flávio Luiz; OLIVEIRA, Luiz Fernando Pinto de. Desenvolvimento De Um Aplicativo No Ambiente App Designer Do Software Matlab® Para Planejamento De Trajetória Do Robô PUMA 560. Engenharia Elétrica e De Computação: Docência, Pesquisa e Inovação Tecnológica 1, no. 1 (2023): 87–109. doi:10.22533/at.ed.4652316018.

[5] ROSSINI, Flávio Luiz; LOPES, João Marcos Periçaro; ABREU, Leonardo de Melo; BARBOSA, Reginaldo Ferreira de Sousa; OLIVEIRA, Luiz Fernando Pinto de. Modelagem, Simulação e Controle De Trajetória Do Robô Manipulador SCARA RS-6 IA Através De Um Aplicativo MATLAB®. Ciências Exatas Estudos e Desafios (V.1) 1 (2022): 30. doi:10.35587/brj.ed.0001995.

[6] ROSSINI, Flávio Luiz. Modelagem Matemática da Dinâmica do Robô Manipulador RC 180, Empresa EPSON, via Formulação Lagrangiana. II Simpósio De Tecnologia e Engenharia Eletrônica - II SIMTEEL, 2014.

[7] MARTINES, Francine; MELO, Larissa; CHICHANOSKI, Gustavo; MUNARINI, Bruno; ROSSINI, Flávio Luiz. Modelagem Matemática da Cinemática Direta do Robô Manipulador SCARA Modelo G-10/G-20. V Ciclo De Palestras: Perspectivas Matemáticas - V CIPEM, 2015.

[8] PENHA, Bruno Schuavab; QUEIROZ, Mariana Emer; ROSSINI, Flávio Luiz. Modelagem e Análise da Cinemática Direta e Inversa de Manipulador Robótico com Cinco Juntas Rotativas. III Simpósio De Tecnologia e Engenharia Eletrônica - III SIMTEEL, 2016.

[9] FUDOLI, Fábio; BLESSA, Lucas; SOUZA, Júlio; ROSSINI, Flávio Luiz. Modelagem Da Cinemática Direta e Inversa Do Robô SCARA EPSON G10-851S. III Simpósio De Tecnologia e Engenharia Eletrônica - III SIMTEEL, 2016.

[10] SANTOS, Matheus Araújo dos; ROSSINI, Flávio Luiz. Modelagem Matemática e Simulação Da Cinemática Direta Do Robô Manipulador Com Seis Juntas Rotativas - 6 GL. III Simpósio De Tecnologia e Engenharia Eletrônica - III SIMTEEL, 2016.

[11] ABREU, Leonardo De Melo; ROSSINI, Flávio Luiz; OLIVEIRA, Luiz Fernando Pinto de. Modelagem Cinemática de um Robô Modelo SCARA e Desenvolvimento de Aplicativo para Análise Gráfica. Anais Do(a) Anais Do XII Seminário De Extensão e Inovação XXVII Seminário De Iniciação Científica e Tecnológica Da UTFPR, n.d. doi:10.29327/1152426.1-2.

[12] OLIVEIRA, L. F. P.; ROSSINI, F. L.; SILVA, M. F.; MOREIRA, A. P. Modeling, Simulation and Implementation of Locomotion Patterns for Hexapod Robots, *2020 IEEE Congreso Bienal de Argentina (ARGENCON)*, Resistencia, Argentina, 2020, pp. 1-1, doi: 10.1109/ARGENCON49523.2020.9505570.

[13] OLIVEIRA, L. F. P.; ROSSINI, F. L. Modeling, Simulation and Analysis of Locomotion Patterns for Hexapod Robots, in *IEEE Latin America Transactions*, vol. 16, no. 2, pp. 375-383, Feb. 2018, doi: 10.1109/TLA.2018.8327389.

[14] SEIKO EPSON CORPORATION. Epson T-Series Robot Manual. Rev. 12, 2020. Disponível em: <https://files.support.epson.com/far/docs/epson _t-series_robot_manual_(r12).pdf> Acessado em 06 de julho de 2022.

[15] UNIVERSIDADE TECNOLÓGICA FEDERAL DO PARANÁ. Coordenação do curso de Engenharia Eletrônica. Disponível em: https://portal.utfpr.edu.br/cursos/coordenacoes/graduacao/campo-mourao/MC-engenharia-eletronica Acessado em 06 de julho de 2022.

[16] CRAIG, J. J.. Robótica. 3ª edição, Pearson Education do Brasil, São Paulo, 2012.

[17] SEIKO EPSON CORPORATION. Robôs SCARA All-In-One Epson Synthis T3. Disponível em <https://epson.com.br/Paraempresas/Rob%C3%B3tica/Rob%C3%B4s-SCARA/Rob%C3%B4sSCARA-All-In-One-Epson-Synthis-T3/p/RT3-401SS.> Acessado em 2 de julho de 2022